phys. stat. sol. (c) 4, No. 12, 4524–4527 (2007) / DOI 10.1002/pssc.200777185

Investigation of sputtered tape media with an ultra-thin magnetic layer

Hwan-Soo Lee* and **David E. Laughlin**

Data Storage Systems Center, Carnegie Mellon University, Pittsburgh, PA 15213, USA

Received 7 May 2007, revised 1 October 2007, accepted 4 Octobr 2007
Published online 18 December 2007

PACS 75.50.Ss, 75.75.+a, 81.15.Cd

Recording characteristics of underlayers (NiAl/CrMn)/intermediate layer (CoCrTa)/CoCrPtBN thin film media sputter-deposited on polymeric substrates were investigated as functions of the magnetic layer and the stack thicknesses. Even a very small thickness of 10 nm of the magnetic layer appeared to be sufficient to preserve the in-plane H_c, and gave rise to the improved recording performances due to primarily the sharper effective head field gradient. The thicknees reduction provided benefits in the fabrication side along with presenting a substantial contribution to the overall recording performance. The overall stack thicknees was reduced down to 70 nm.

1 Introduction

Along with the advanced metal particle (MP) or advanced metal evaporated (ME) tape media, sputtered media can offer very promising long term solution as the next generation tape media [1–3]. Previously, NiAl/CrMn underlayers (ULs) and CoCrTa intermediate layer (IL) were used in order to induce a smaller grain size and better promote epitaxial growth of the hcp structure [4]. However, the film structure is relatively complex and expensive to commercialize. Ultimately, for this technology to be transferred to tape media application, reducing the thickness provides benefits not only in the recording side but also in the fabrication side.

In this study, the effects of media thickness on recording performances were investigated. Additionally, a reduction in the stack thickness was discussed, in the context of the need to reduce deposition dwell time in sputtered tape manufacturing.

2 Experimental

Films of CoCrPtBN with various thicknesses were sputter-deposited on either glass or advanced ARAMID tape substrates (average roughness, R_a = 1.4 nm for tape). A CoCrPt alloy target with Pt and BN chips was for magnetic film preparation. The underlayer stack used to produce the in-plane texture was substrate/NiAl/CrMn/CoCrTa as reported previously [4]. The CoCrTa composition is high enough in Cr that the alloy is non-magnetic. The thicknesses of the three non-magnetic layers were NiAl (60nm)/CrMn (30nm)/CoCrTa (8 nm), and the thickness of the CoCrPtBN magnetic layer was 16 nm unless stated otherwise. Other details of the sputtering conditions are described elsewhere [4].

Magnetic properties of the samples were measured by an alternating gradient magnetometer (AGM) and a vibrating sample magnetometer (VSM). Film textures and microstructures were characterized by

* Corresponding author: e-mail: hwansoo@ece.cmu.edu, Phone: +1 412 268 4034, Fax: +1 412 268 6978

an X-ray diffractometer (Philips X'pert Pro with X-ray lens) using Cu K_α radiation and by a transmission electron microscope (TEM) operating at 200 kV.

For protecting the head-tape interface during recording measurements, carbon nitride (CNx) overcoats were reactively deposited using an Anelva SPF-730 sputtering system. The recording measurements were carried out on a drum tester at a head-medium velocity of 6.8 m/s, using a metal-in-gap (MIG) write head with an effective gap length of 0.2 μm and a track width of 17 μm, and an anisotropic magnetoresistive (AMR) read head with a shield-to-shield distance of 0.23 μm and a track width of 7 μm. The sense current of the AMR head was 10 mA. The resolution bandwidth (RBW) for the measurement was chosen to be 30 kHz for the spectral analysis.

3 Results and discussion

3.1 Media fabrication

Figures 1(a-d) show thickness dependence of the three non-magntic layers as well as the CoCrPtBN magnetic layer on coercivity, H_c of the CoCrPtBN films. Glass substrates were initially used as a standard substrate because they can make the process simple with better reproducibility. The dotted lines indicate the minimum thickness for each layer to sustain H_c without degradation. The minimum thicknesses for NiAl, CrMn, CoCrTa, and CoCrPtBN are 45, 6, 4, and 10 nm, respectively. Note that the NiAl layer largely determines the deposition dwell time. The NiAl underlayer needs to be thick enough to preserve the in-plane H_c. In-plane orientation (10.0) of the CoCrPtBN can be obtained by the epitaxial relationship between NiAl (112)/Cr (112) and CoCrTa (10.0)/CoCrPtBN (10.0).

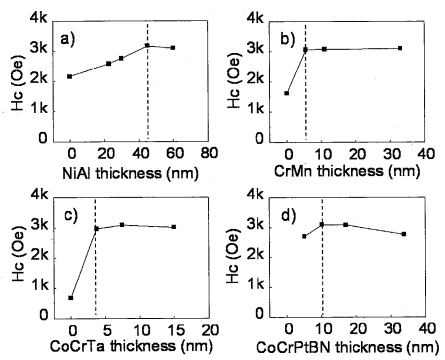

Fig. 1 H_c as functions of a) NiAl, b) CrMn, c) CoCrTa, and d) CoCrPtBN thicknesses. The reference stack structure: glass/NiAl (60nm)/CrMn (30nm)/CoCrTa (8nm)/CoCrPtBN (16nm).

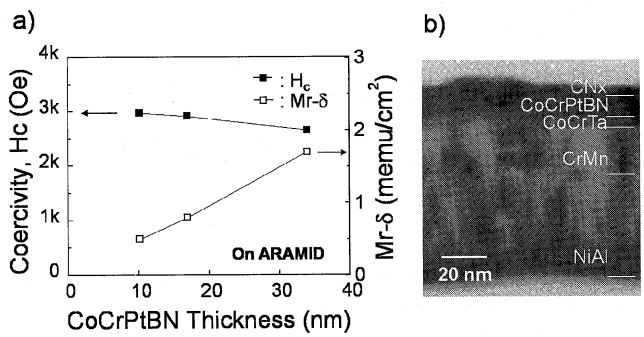

Fig. 2 (a) Coercivity (H_c) and Mr-δ as a function of the CoCrPtBN thickness (δ). The samples were deposited on polymeric substrates (ARAMID). (b) Cross-sectional image of a sample stack.

A similar series of samples was also deposited on polymeric substrates (ARAMID). In Fig. 2, H_c is shown as a function of the CoCrPtBN thickness. The thicknesses of the three non-magnetic layers were chosen (from Fig. 1) not to degrade the coercivity of the CoCrPtBN films. The thicknesses of the NiAl, CrMn, and CoCrTa layers were 40, 20, and 4, respectively. Consistent with Fig. 1(d), reducing the magnetic layer thickness down to 10 nm resulted in an increase in H_c. The H_c values increased from 2650 to 2970 Oe as the CoCrPtBN thicknesses (δ) decreased from 34 to 10 nm. The measured Mr·δ changed from 1.7 to 0.5 memu/cm^2. In Fig. 2(b), a cross-sectional TEM of a sample stack is shown. The atomic registry across the boundaries is evident in the image. The grain-to-grain growth at the NiAl/CrMn interface can be also seen as indicated by arrows. The overall thickness of the stack is about 70 nm.

3.2 Recording characteristics

Figure 3 shows signal-to-noise ratio (SNR) as a function of recording density for two stacks A and B, which were fabricated with different layer thicknesses. The thickness of the underlayers (ULs, Ni-Al/CrMn) in stack A is 55 nm whereas that in stack B is 90 nm (see the insets). The overall thickness of stack A was nearly halved comparing to that of stack B. Note also that stack B has no CNx overcoat.

In the figure, an improvement in SNR for stack A by employing the thinner magnetic layer (9nm) is unambiguous. SNR of stack A is 4 dB higher than that of stack B at a linear density of 140 kfci. The improvement in SNR seems to arise from the thinner magnetic layer for stack A. Possible causes to vary average spacing can be surface topography, the head contour or the tape rigidity. However, the testing conditions were identical and the other factors were nearly the same. Grain size was slightly smaller for stack A, which, not primarily, but may contribute to the observed change in SNR.

For direct comparison, SNR was estimated by assuming a 5 nm thick overcoat for stack B. The dotted line in the figure corresponds to the case that the overcoat would be present. Loss factor, $-99(d/\lambda)$ in dB during write/read processes was taken into account for the computation [5]. The d and λ represent the head-medium spacing and the recorded wavelength, respectively. Note that higher frequency content for stack A attenuates more even when the CNx layer was assumed for stack B (see the dotted line). This may indicate additional factors other than spacing is important at high frequency.

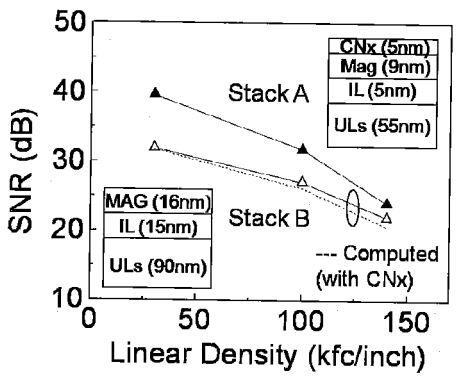

Fig. 3 Signal-to-noise ratio (SNR) with respect to linear density. Note the overall thickness of stack A is nearly halved in comparison with that of stack B.

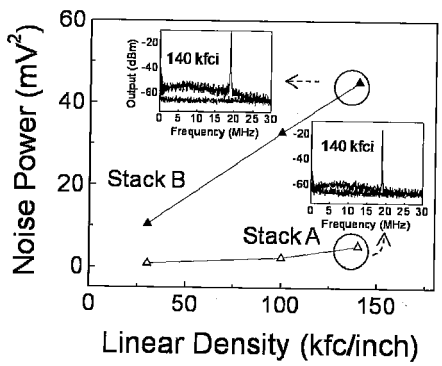

Fig. 4 Integrated noise power with respect to recording density for stacks A and B. The insets show the spectra of signal and noise at a linear density of 140 kfci.

In Fig. 4, integrated noise power for stack A and B is shown with respect to recording density. The media noise of stack A was apparently smaller. The insets represent the spectra of signal and noise for stacks A and B at a linear density of 140 kfci. The media noise of stack A is shown to be lower by about 5 dB at low frequency range than that for stack B. Electronic noise floor is also shown for the both stacks.

In Fig. 5(a), the isolated readback pulses for stacks A and B are shown. A pulse width at 50% of maximum amplitude (PW_{50}) of stack A is 18% narrower, showing 21% smaller in magnitude than that of stack B. We estimate from the observed PW_{50} that the transition parameter a becomes narrower by about 30% for stack A. (The corresponding channel density, D_{50} (the density which produced 50% of the maximum output voltage) of stack A was observed to be 157 kfci, but a damage for stack B occurred during measurement made the comparison incomplete in terms of D_{50}).

On a closer look, there is an asymmetry of the baseline on either side of the isolated peak. Perpendicular components of magnetization can be a cause of the asymmetry in the reproduced signal [6]. In Fig. 5(b), for various tape samples, the asymmetry associated with magnetization (M_θ) at an angle θ to the tape plane (see the inset) was correlated to the measured c-axis (easy axis) out-of-plane components. The

intensity ratio (R) of the in-plane I(10.0) and out-of-plane I(00.2) components, where I_{hkl} is the (hkl) intensity, was determined by the corresponding x-ray diffraction spectra (XRD). If the ratio R becomes smaller, the easy axes of grains are more randomly distributed within the film, which in turn leads to the lower anisotropy energy. Consequently, the ratio R can be important in determining the recording characteristics such as linear density, SNR and etc. As the texture was properly controlled (R > 1.5), asymmetry was less than 3%.

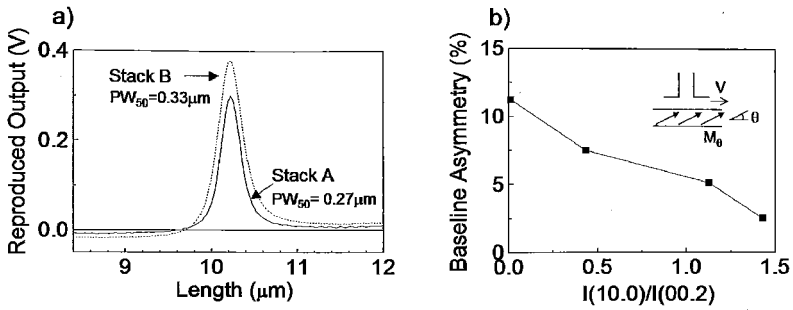

Fig. 5 (a) Isolated pulse of reproduced output signal for stacks A and B. The CoCrPtBN thicknesses are 9 nm and 16 nm, respectively. (b) Asymmetry of the baseline on either side of the isolated peak versus ratio of the in-plane I(10.0) and out-of-plane I(00.2) components determined by XRD spectra. The inset illustrates easy axis at an angle θ to the tape plane where V is the head-medium velocity.

The frequency response is primarily determined by the recorded transition width parameter (a). The transition width may be composed of the medium parameter (a_m), which is related to grain size and a degree in exchange coupling in the medium, and the head parameter (a_h), which is mainly related to a sharpness in head field gradient. Intergranular exchange interaction is often seen to play a key role in reducing the media noise, however, the observed difference between stacks A and B is not likely to root from a_m since similar exchange coupling ($\Delta M_{max} \sim 0.24$) was observed. Rather, the contribution of a_h caused by a reduction in medium thickness, is understood to be important in the first place. We attribute the reduced transition length and noise to the improved *effective* head field gradient at a smaller medium thickness. This allows the resulting sharper transition to encompass fewer grains, and thus fewer noise sources.

4 Conclusions

Sputtered tape media possessing a very thin magnetic layer (which is typical in hard disk media) has been investigated. The sharper transition obtained by reducing the recording layer thickness accounted for the observed improvements in recording characteristics. Engineering the magnetic layer thickness and the underlayers thickness can permit the benefit in a view of not only practical fabrication but recording performances.

Acknowledgements One of the authors gratefully acknowledges the Advanced Media Development of Sony Corporation (Sony Sendai) for their technical assistance, and Prof. Jian-Gang Zhu for travel support.

References

[1] H.-S. Lee, D. E. Laughlin, and J. A. Bain, IEEE Trans. Magn. **40**, 2404 (2004).
[2] K. Moriwaki, K. Usuki, and M. Nagao, IEEE Trans. Magn. **41**, 3244 (2005).
[3] H. Fujiura and S. Nakagawa, J. Magn. Magn. Mater. **310**, 2659 (2007).
[4] H.-S. Lee, L. Wang, J. A. Bain, and D. E. Laughlin, IEEE Trans. Magn. **39**, 3616 (2003).
[5] H.-S. Lee, J. A. Bain, and D. E. Laughlin, IEEE Trans. Magn. **41**, 2529 (2005).
[6] B. K. Middleton, C. D. Wright, S. R. Cumpson, and J. J. Miles, IEEE Trans. Magn. **31**, 2365 (1995).